Supplementary material (ESI) for Journal of Materials Chemistry

Electronic Supplementary Information (ESI)

Impact of core chirality on mesophase properties of perylene bisimides

Marina M. Safont-Sempere, Vladimir Stepanenko, Matthias Lehmann* and Frank Würthner*

Universität Würzburg, Institut für Organische Chemie and Röntgen Research Center for Complex Material Systems, Am Hubland, 97074 Würzburg, Germany.

E-mail: wuerthner@chemie.uni-wuerzburg.de

E-mail: matthias.lehmann@ uni-wuerzburg.de

Table of Contents:

1. ***Polarization microscope studies***

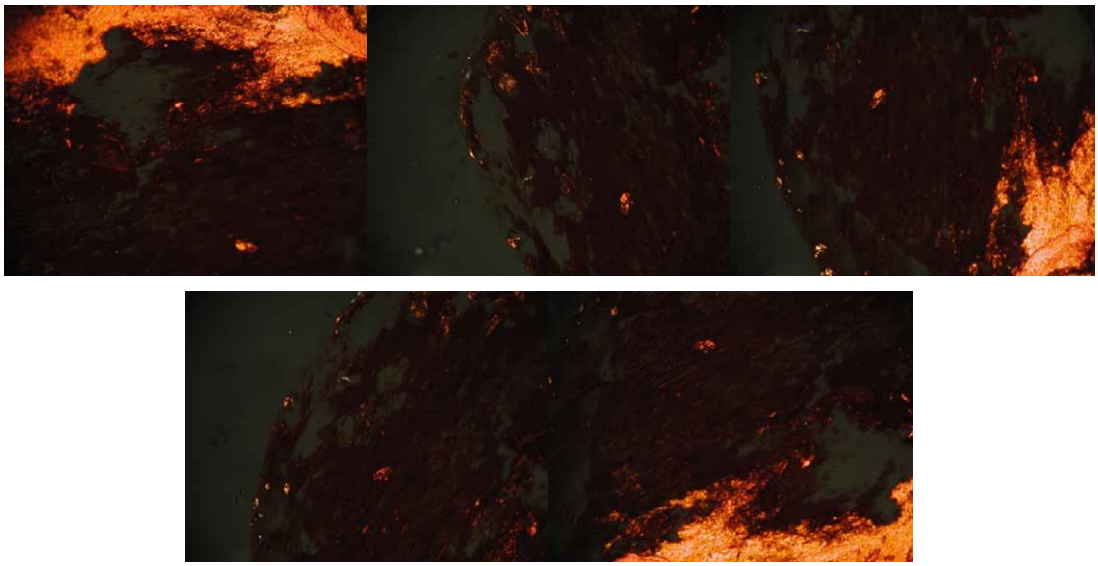

Figure S1. Pictures of a sheared sample of (*M*)-**1** at different rotation angles respective to the light beam in the polarization microscope with the polarizator in perpendicular mode.

2. ***Model of the Soft Crystalline Columnar Phase***

The model of the soft crystal phase was created with the software package Materials Studio (Accelrys). The geometry energy minimization and annealing procedures were performed with the force field module Forcite Plus (COMPASS). First, a single stack of four PBI mesogens *MPPM* was assembled which were perfectly aligned, placed in a large orthorhombic cell and the cell parameters *a/2* and *c* were slowly adjusted to the experimental values, while optimizing the geometry of the assembly. During this procedure, the PBIs which are slightly rotated to each other in the π-stack remained at their positions and mainly the bridges and dodecyl chains optimized for packing and space filling. Subsequently, the cell was enlarged by the factor of two from *a*/2 to *a* and the value for parameter *b* was selected that a second *MPPM* stack did not experience any steric interaction with the first, when the assemblies were positioned at x = *a*/4 and y = *b*/4 for the first and x = 3*a*/4 and y = 3*b*/4 for the second column. Before *b* was now stepwise reduced, two lateral aliphatic chains were folded back from each molecule to fill the space along the long axis of the PBIs. Thus, in total 16 of 48 chains are folded in that way in order to reduce the steric interaction and hence to maintain a high order of the aliphatic chains when the cell size is reduced. The parameter *b* was then stepwise reduced by 2 Å and in each step the cell was geometry optimized (500 iterations). The stacks were positioned in order to maintain the centered rectangular order,

before *b* was reduced again until the experimental value was obtained. The final cell was geometry optimized until a minimum was reached. Subsequently, a supercell (2*a*, 2*b*, *c*) containing four unit cells was formed and exposed to five annealing cycles between 300 K and 700 K for a total of 50ps. The structure was again geometry minimized until the calculation did converge.

3. ***Interpretation of the X-ray pattern of the soft columnar crystal at 149 °C***

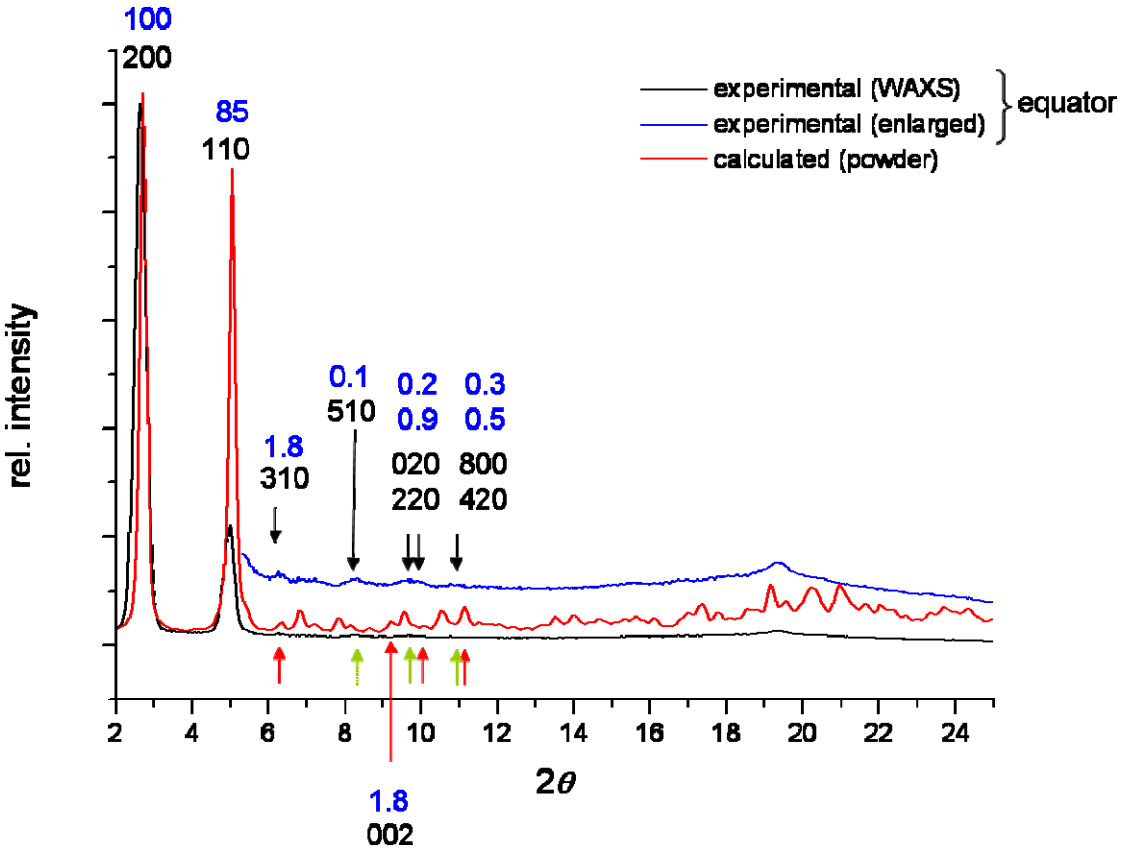

Figure S2. Experimental X-ray pattern integrated along the equator (black and wide angle interval enlarged in blue) and the calculated powder pattern of a model. Numbers in black are the Miller indices and the numbers in blue the relative intensities from the calculated pattern.

Figure S2 shows the calculated X-ray powder diffraction pattern in comparison with the integration of the experimental pattern along the equator. The equatorial signals (200 and 110) are the only intense reflections and the large arcs show a considerable amount of misalignment. The relatively large number of meridional and equatorial reflections points to a crystal phase, however, the shearability and disorder let us classify this phase as a soft crystal. The structure shown in Figure 6 (in the paper) takes into account all these features. The corresponding powder X-ray diffraction can be, however, only qualitatively compared to the

experimental pattern. It was not our intension to fit the experiment, which is not possible due to the soft nature of the phase and the high disorder, but instead we sought to rationalize qualitatively our interpretation of the obtained low quality diffraction pattern. Indeed, only the 200 and 110 reflections are very strong for the model. All other reflections are below 2% and most of them are even below 1% of the intensity of the highest reflection (100%). Among the most prominent of the low intensity reflections is the 002 which is three times more intense than the 001, the latter is not detected in the experimental pattern, most probably because it is covered by the 110 signal of the misaligned columnar phase. However, the diffuse 002 reflection is clearly visible. Other relatively large signals present in the experimental pattern are the 310 and the 420 reflections.

Reflections which are not yet well understood represent the more intense diffuse intensity superimposed on the halo at 4.5 Å, which we relate to a fraction of aliphatic chains which are more ordered than the disordered liquid aliphatic chains which we attribute to the diffuse broad intensity at 4.6 Å (Figure S3). A further diffraction is located at the meridian at 5.1 Å between the reflections 002 and 004. However, at this position no reflection is expected for an orthorhombic soft crystal. Even for the partially aligned fiber in the present experiment, reflections hk1, hk2, hk3, hk4, … , hkl should appear at defined layer lines. The intensity at 5.1 Å at the meridian cannot be assigned to a layer line but might be attributable to the distance between two PBI dyes separated by the oligoethylene glycol bridges along the column (Figure S4).

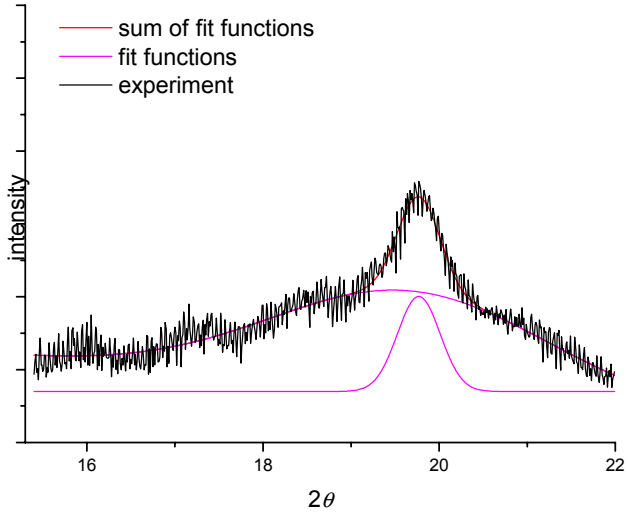

Figure S3. Experimental X-ray pattern integrated along the equator (black and WAXS) and fit functions (violet line).

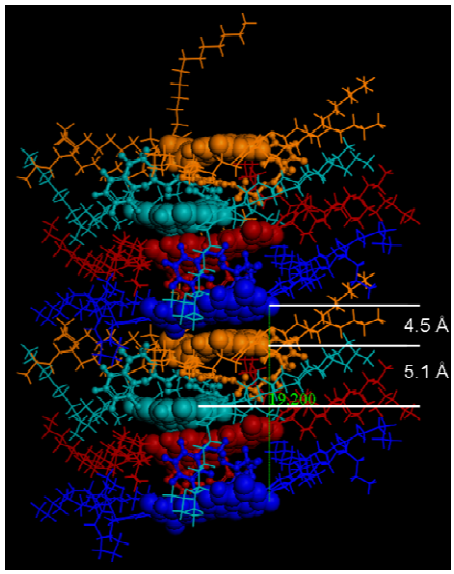

Figure S4. Columnar stack showing the 5.1 Å distance, which presumably has its origin in two aromatic entities separated by the bridges.

Eventually, it could be argued that the relatively low quality of the diffraction pattern might be due to an inhomogeneous sample, that is, a mixture of liquid and crystalline sample. However, this can be ruled out since the X-ray pattern was collected at 149 °C whereas the transition is well defined above 240 °C. Moreover, the pattern remained almost unchanged upon further cooling to 30 °C (Figure S5).

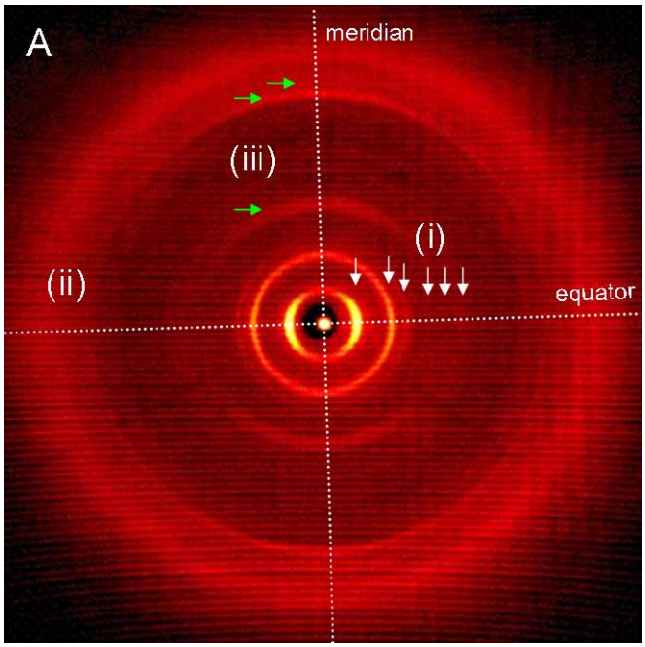

Figure S5. Diffraction pattern of the racemic PBI **1** at 30 °C. The pattern is very similar to the one at 149 °C with reflections (i) at the equator (white arrows), halo (ii) and meridional reflections (iii) (green arrows).

4. ***Circular dichroism (CD) studies***

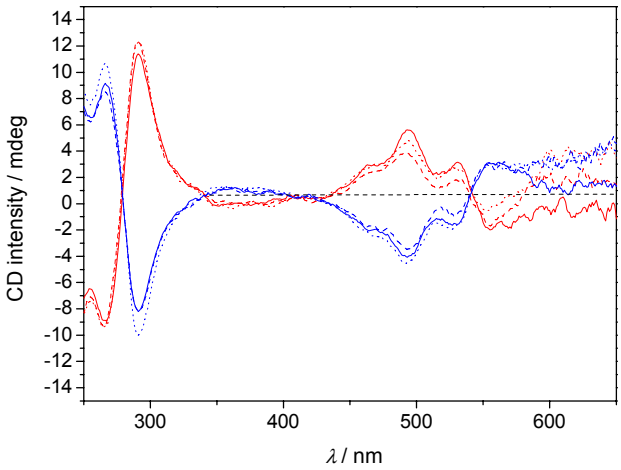

Figure S6. CD spectra of thin films of (*P*)-**1** (red line) and (*M*)-**1** (blue line) measured perpendicular to the light beam at three different angles: 0° (solid line), 45° (dashed line) and 90° (dotted line).

5. ***Elasticity modulus determination by AFM***

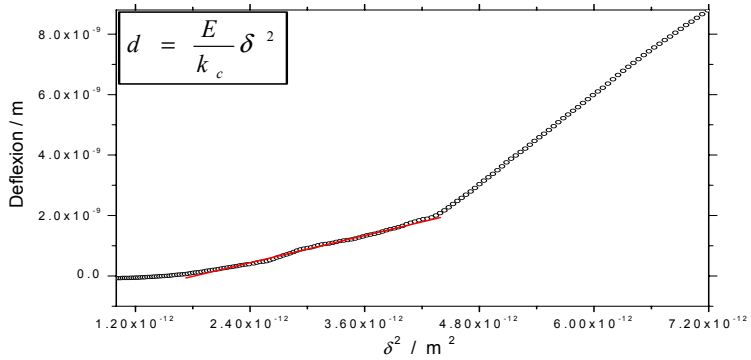

Figure S7. Deflection of the AFM tip as a function of the square of the indentation depth for (*rac*)-**1** and corresponding applied equation for obtaining the elasticity module, where d is the vertical displacement of the cantilever, k_C is the stiffness of the cantilever, δ is the indentation depth and E is the elasticity module.